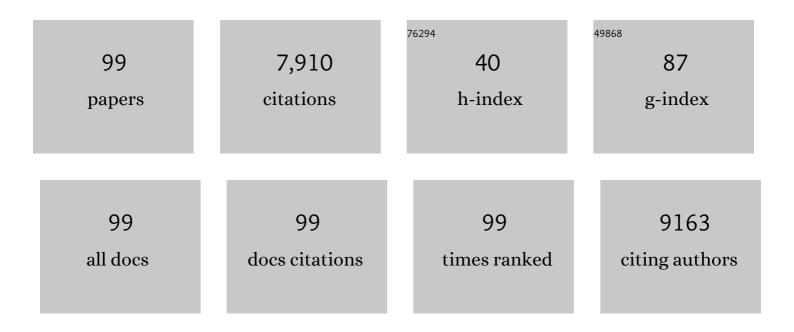
Jianshe Liu

List of Publications by Year in descending order

Source: https://exaly.com/author-pdf/3200425/publications.pdf Version: 2024-02-01



#	Article	IF	CITATIONS
1	Facile construction of novel organic–inorganic tetra (4-carboxyphenyl) porphyrin/Bi2MoO6 heterojunction for tetracycline degradation: Performance, degradation pathways, intermediate toxicity analysis and mechanism insight. Journal of Colloid and Interface Science, 2022, 605, 727-740.	5.0	176
2	Fabrication of NH2-MIL-125(Ti) nanodots on carbon fiber/MoS2-based weavable photocatalysts for boosting the adsorption and photocatalytic performance. Journal of Colloid and Interface Science, 2022, 611, 706-717.	5.0	43
3	Performance of UV/acetylacetone process for saline dye wastewater treatment: Kinetics and mechanism. Journal of Hazardous Materials, 2021, 406, 124774.	6.5	17
4	BiOBr/Ag/AgBr heterojunctions decorated carbon fiber cloth with broad-spectral photoresponse as filter-membrane-shaped photocatalyst for the efficient purification of flowing wastewater. Journal of Colloid and Interface Science, 2021, 587, 633-643.	5.0	45
5	TiO2/BiOI p-n junction-decorated carbon fibers as weavable photocatalyst with UV–vis photoresponsive for efficiently degrading various pollutants. Chemical Engineering Journal, 2021, 415, 129019.	6.6	130
6	Decoration of amine functionalized zirconium metal organic framework/silver iodide heterojunction on carbon fiber cloth as a filter- membrane-shaped photocatalyst for degrading antibiotics. Journal of Colloid and Interface Science, 2021, 603, 582-593.	5.0	20
7	Co-metabolic degradation of refractory dye: A metagenomic and metaproteomic study. Environmental Pollution, 2020, 256, 113456.	3.7	26
8	A novel 3D Z-scheme heterojunction photocatalyst: Ag ₆ Si ₂ O ₇ anchored on flower-like Bi ₂ WO ₆ and its excellent photocatalytic performance for the degradation of toxic pharmaceutical antibiotics. Inorganic Chemistry Frontiers, 2020, 7, 529-541.	3.0	121
9	Is addition of reductive metals (Mo, W) a panacea for accelerating transition metals-mediated peroxymonosulfate activation?. Journal of Hazardous Materials, 2020, 386, 121877.	6.5	44
10	Construction of titanium dioxide/cadmium sulfide heterojunction on carbon fibers as weavable photocatalyst for eliminating various contaminants. Journal of Colloid and Interface Science, 2020, 561, 307-317.	5.0	39
11	Fabrication of MoS ₂ /BiOBr heterojunctions on carbon fibers as a weaveable photocatalyst for tetracycline hydrochloride degradation and Cr(<scp>vi</scp>) reduction under visible light. Environmental Science: Nano, 2020, 7, 2708-2722.	2.2	47
12	Construction of TiO2/Ag3PO4 nanojunctions on carbon fiber cloth for photocatalytically removing various organic pollutants in static or flowing wastewater. Journal of Colloid and Interface Science, 2020, 571, 213-221.	5.0	50
13	Spatial and seasonal variations and risk assessment for heavy metals in surface sediments of the largest river-embedded reservoir in China. Environmental Science and Pollution Research, 2020, 27, 35556-35566.	2.7	13
14	The key factors and removal mechanisms of sulfadimethoxazole and oxytetracycline by coagulation. Environmental Science and Pollution Research, 2020, 27, 16167-16176.	2.7	9
15	Construction of n-TiO2/p-Ag2O Junction on Carbon Fiber Cloth with Vis–NIR Photoresponse as a Filter-Membrane-Shaped Photocatalyst. Advanced Fiber Materials, 2020, 2, 13-23.	7.9	126
16	Deciphering the mechanism of carbon sources inhibiting recolorization in the removal of refractory dye: Based on an untargeted LC–MS metabolomics approach. Bioresource Technology, 2020, 307, 123248.	4.8	12
17	The enhanced degradation and detoxification of chlortetracycline by Chlamydomonas reinhardtii. Ecotoxicology and Environmental Safety, 2020, 196, 110552.	2.9	20
18	Tea Residue Boosts Dye Decolorization and Induces the Evolution of Bacterial Community. Water, Air, and Soil Pollution, 2019, 230, 1.	1.1	3

#	Article	IF	CITATIONS
19	Sugar sources as Co-substrates promoting the degradation of refractory dye: A comparative study. Ecotoxicology and Environmental Safety, 2019, 184, 109613.	2.9	16
20	An often-overestimated adverse effect of halides in heat/persulfate-based degradation of wastewater contaminants. Environment International, 2019, 130, 104918.	4.8	36
21	Unveiling the activating mechanism of tea residue for boosting the biological decolorization performance of refractory dye. Chemosphere, 2019, 233, 110-119.	4.2	12
22	Chlorine incorporation into dye degradation by-product (coumarin) in UV/peroxymonosulfate process: A negative case of end-of-pipe treatment. Chemosphere, 2019, 229, 374-382.	4.2	25
23	Synthesis of MoS ₂ /CdS Heterostructures on Carbonâ€Fiber Cloth as Filterâ€Membraneâ€6haped Photocatalyst for Purifying the Flowing Wastewater under Visibleâ€Light Illumination. ChemCatChem, 2019, 11, 2855-2863.	1.8	49
24	Facile construction of flower-like bismuth oxybromide/bismuth oxide formate p-n heterojunctions with significantly enhanced photocatalytic performance under visible light. Journal of Colloid and Interface Science, 2019, 548, 12-19.	5.0	92
25	Fructose as an additional co-metabolite promotes refractory dye degradation: Performance and mechanism. Bioresource Technology, 2019, 280, 430-440.	4.8	35
26	Removal of active dyes by ultrafiltration membrane pre-deposited with a PSFM coagulant: Performance and mechanism. Chemosphere, 2019, 223, 204-210.	4.2	16
27	Facile Fabrication of Flower-Like BiOI/BiOCOOH p–n Heterojunctions for Highly Efficient Visible-Light-Driven Photocatalytic Removal of Harmful Antibiotics. Nanomaterials, 2019, 9, 1571.	1.9	7
28	Preparation and evaluation of a hierarchical Bi ₂ MoO ₆ /MSB composite for visible-light-driven photocatalytic performance. RSC Advances, 2019, 9, 38280-38288.	1.7	8
29	MoS2/Bi2S3 heterojunctions-decorated carbon-fiber cloth as flexible and filter-membrane-shaped photocatalyst for the efficient degradation of flowing wastewater. Journal of Alloys and Compounds, 2019, 779, 599-608.	2.8	51
30	Visâ€NIR Lightâ€Responsive Photocatalytic Activity of C ₃ N ₄ â^'Agâ^'Ag ₂ O Heterojunctionâ€Decorated Carbonâ€fiber Cloth as Efficient Filterâ€Membraneâ€Shaped Photocatalyst. ChemCatChem, 2019, 11, 1362-1373.	1.8	38
31	Electroactive Modified Carbon Nanotube Filter for Simultaneous Detoxification and Sequestration of Sb(III). Environmental Science & Technology, 2019, 53, 1527-1535.	4.6	111
32	Performance and microbial protein expression during anaerobic treatment of alkali-decrement wastewater using a strengthened circulation anaerobic reactor. Bioresource Technology, 2019, 273, 40-48.	4.8	3
33	On peroxymonosulfate-based treatment of saline wastewater: when phosphate and chloride co-exist. RSC Advances, 2018, 8, 13865-13870.	1.7	26
34	Peroxymonosulfate/base process in saline wastewater treatment: The fight between alkalinity and chloride ions. Chemosphere, 2018, 199, 84-88.	4.2	93
35	Illumina MiSeq sequencing reveals microbial community in HA process for dyeing wastewater treatment fed with different co-substrates. Chemosphere, 2018, 201, 578-585.	4.2	39
36	Preparation and properties of chitosan–metal complex: Some factors influencing the adsorption capacity for dyes in aqueous solution. Journal of Environmental Sciences, 2018, 66, 301-309.	3.2	48

#	Article	IF	CITATIONS
37	Smartphoneâ€based colorimetric chiral recognition of ibuprofen using aptamersâ€capped gold nanoparticles. Electrophoresis, 2018, 39, 486-495.	1.3	22
38	Synthesis of Flower-Like AgI/BiOCOOH p-n Heterojunctions With Enhanced Visible-Light Photocatalytic Performance for the Removal of Toxic Pollutants. Frontiers in Chemistry, 2018, 6, 518.	1.8	18
39	Facile Synthesis of Bi2MoO6 Microspheres Decorated by CdS Nanoparticles with Efficient Photocatalytic Removal of Levfloxacin Antibiotic. Catalysts, 2018, 8, 477.	1.6	11
40	Iron Plaque: A Barrier Layer to the Uptake and Translocation of Copper Oxide Nanoparticles by Rice Plants. Environmental Science & Technology, 2018, 52, 12244-12254.	4.6	74
41	Hierarchical heterostructures of Bi2MoO6 microflowers decorated with Ag2CO3 nanoparticles for efficient visible-light-driven photocatalytic removal of toxic pollutants. Beilstein Journal of Nanotechnology, 2018, 9, 2297-2305.	1.5	15
42	Treatment of industrial dyeing wastewater with a pilot-scale strengthened circulation anaerobic reactor. Bioresource Technology, 2018, 264, 154-162.	4.8	63
43	Facile synthesis of cerium oxide nanoparticles decorated flower-like bismuth molybdate for enhanced photocatalytic activity toward organic pollutant degradation. Journal of Colloid and Interface Science, 2018, 530, 171-178.	5.0	167
44	Ag ₂ WO ₄ nanorods decorated with AgI nanoparticles: Novel and efficient visible-light-driven photocatalysts for the degradation of water pollutants. Beilstein Journal of Nanotechnology, 2018, 9, 1308-1316.	1.5	22
45	Facile Preparation of Nano-Bi2MoO6/Diatomite Composite for Enhancing Photocatalytic Performance under Visible Light Irradiation. Materials, 2018, 11, 267.	1.3	19
46	Ag3VO4 Nanoparticles Decorated Bi2O2CO3 Micro-Flowers: An Efficient Visible-Light-Driven Photocatalyst for the Removal of Toxic Contaminants. Frontiers in Chemistry, 2018, 6, 255.	1.8	37
47	Comparative study of antiestrogenic activity of two dyes after Fenton oxidation and biological degradation. Ecotoxicology and Environmental Safety, 2018, 164, 416-424.	2.9	31
48	Deciphering the degradation/chlorination mechanisms of maleic acid in the Fe(II)/peroxymonosulfate process: An often overlooked effect of chloride. Water Research, 2018, 145, 453-463.	5.3	73
49	Preparation of TiO2/C3N4 heterojunctions on carbon-fiber cloth as efficient filter-membrane-shaped photocatalyst for removing various pollutants from the flowing wastewater. Journal of Colloid and Interface Science, 2018, 532, 798-807.	5.0	85
50	Significantly enhanced base activation of peroxymonosulfate by polyphosphates: Kinetics and mechanism. Chemosphere, 2017, 173, 529-534.	4.2	96
51	Facile synthesis of Fe 2 O 3 nanoparticles anchored on Bi 2 MoO 6 microflowers with improved visible light photocatalytic activity. Journal of Colloid and Interface Science, 2017, 497, 93-101.	5.0	96
52	Facile synthesis of flower-like Ag 3 VO 4 /Bi 2 WO 6 heterojunction with enhanced visible-light photocatalytic activity. Journal of Colloid and Interface Science, 2017, 501, 156-163.	5.0	152
53	Construction of fiber-shaped silver oxide/tantalum nitride p-n heterojunctions as highly efficient visible-light-driven photocatalysts. Journal of Colloid and Interface Science, 2017, 504, 561-569.	5.0	64
54	Trace bromide ion impurity leads to formation of chlorobromoaromatic by-products in peroxymonosulfate-based oxidation of chlorophenols. Chemosphere, 2017, 182, 624-629.	4.2	16

#	Article	IF	CITATIONS
55	On the kinetics of organic pollutant degradation with Co2+/peroxymonosulfate process: When ammonium meets chloride. Chemosphere, 2017, 179, 331-336.	4.2	37
56	Both degradation and AOX accumulation are significantly enhanced in UV/peroxymonosulfate/4-chlorophenol/Cl ^{â^'} system: two sides of the same coin?. RSC Advances, 2017, 7, 12318-12321.	1.7	33
57	Seawater desalination with solar-energy-integrated vacuum membrane distillation system. Journal of Water Reuse and Desalination, 2017, 7, 16-24.	1.2	6
58	Synthesis of Ta ₃ N ₅ /Bi ₂ MoO ₆ core–shell fiber-shaped heterojunctions as efficient and easily recyclable photocatalysts. Environmental Science: Nano, 2017, 4, 1155-1167.	2.2	180
59	Biopolymer-induced morphology control of brushite for enhanced defluorination of drinking water. Journal of Colloid and Interface Science, 2017, 491, 207-215.	5.0	15
60	Effects of chloride on PMS-based pollutant degradation: A substantial discrepancy between dyes and their common decomposition intermediate (phthalic acid). Chemosphere, 2017, 187, 338-346.	4.2	45
61	Chemical instability of graphene oxide following exposure to highly reactive radicals in advanced oxidation processes. Journal of Colloid and Interface Science, 2017, 507, 51-58.	5.0	20
62	Performance and microbial community structures of hydrolysis acidification process treating azo and anthraquinone dyes in different stages. Environmental Science and Pollution Research, 2017, 24, 252-263.	2.7	28
63	A Novel Heterostructure of BiOI Nanosheets Anchored onto MWCNTs with Excellent Visible-Light Photocatalytic Activity. Nanomaterials, 2017, 7, 22.	1.9	45
64	Transformation of CuO Nanoparticles in the Aquatic Environment: Influence of pH, Electrolytes and Natural Organic Matter. Nanomaterials, 2017, 7, 326.	1.9	89
65	Al-Doped chitosan nonwoven in a novel adsorption reactor with a cylindrical sleeve for dye removal: performance and mechanism of action. RSC Advances, 2016, 6, 110935-110942.	1.7	7
66	High Efficiency CdS/CdSe Quantum Dot Sensitized Solar Cells with Two ZnSe Layers. ACS Applied Materials & Interfaces, 2016, 8, 34482-34489.	4.0	85
67	A comparison of ZnS and ZnSe passivation layers on CdS/CdSe co-sensitized quantum dot solar cells. Journal of Materials Chemistry A, 2016, 4, 14773-14780.	5.2	70
68	Synthesis of BiOBr/WO ₃ p–n heterojunctions with enhanced visible light photocatalytic activity. CrystEngComm, 2016, 18, 3856-3865.	1.3	104
69	Is UV/Ce(iv) process a chloride-resistant AOPs for organic pollutants decontamination?. RSC Advances, 2016, 6, 93558-93563.	1.7	7
70	Importance of reagent addition order in contaminant degradation in an Fe(<scp>ii</scp>)/PMS system. RSC Advances, 2016, 6, 70271-70276.	1.7	39
71	Comparison of UV/hydrogen peroxide and UV/peroxydisulfate processes for the degradation of humic acid in the presence of halide ions. Environmental Science and Pollution Research, 2016, 23, 4778-4785.	2.7	42
72	Characteristics of estrogenic/antiestrogenic activities during the anoxic/aerobic biotreatment process of simulated textile dyeing wastewater. RSC Advances, 2016, 6, 25624-25632.	1.7	7

#	Article	IF	CITATIONS
73	Visible-light-driven photocatalytic inactivation of Escherichia coli by magnetic Fe2O3–AgBr. Water Research, 2016, 90, 111-118.	5.3	106
74	Enhanced AOX accumulation and aquatic toxicity during 2,4,6-trichlorophenol degradation in a Co(II)/peroxymonosulfate/Clâ°' system. Chemosphere, 2016, 144, 2415-2420.	4.2	72
75	Transformations of chloro and nitro groups during the peroxymonosulfate-based oxidation of 4-chloro-2-nitrophenol. Chemosphere, 2015, 134, 446-451.	4.2	100
76	Coprecipitated arsenate inhibits thermal transformation of 2-line ferrihydrite: Implications for long-term stability of ferrihydrite. Chemosphere, 2015, 122, 88-93.	4.2	38
77	Fe2O3–AgBr nonwoven cloth with hierarchical nanostructures as efficient and easily recyclable macroscale photocatalysts. RSC Advances, 2015, 5, 10951-10959.	1.7	34
78	Fe-catalyzed photoreduction of Cr(VI) with dicarboxylic acid (C ₂ –C ₅): divergent reaction pathways. Desalination and Water Treatment, 2015, 56, 1020-1028.	1.0	7
79	Enhanced catalytic ability of chitosan–Cu–Fe bimetal complex for the removal of dyes in aqueous solution. RSC Advances, 2015, 5, 90731-90741.	1.7	58
80	Flower-like Bi ₂ S ₃ /Bi ₂ MoO ₆ heterojunction superstructures with enhanced visible-light-driven photocatalytic activity. RSC Advances, 2015, 5, 75081-75088.	1.7	78
81	Characteristics, Process Parameters, and Inner Components of Anaerobic Bioreactors. BioMed Research International, 2014, 2014, 1-10.	0.9	71
82	Distinct effects of oxalate versus malonate on the iron redox chemistry: Implications for the photo-Fenton reaction. Chemosphere, 2014, 103, 354-358.	4.2	26
83	A novel photosensitized Fenton reaction catalyzed by sandwiched iron in synthetic nontronite. RSC Advances, 2014, 4, 12958.	1.7	30
84	Diverse redox chemistry of photo/ferrioxalate system. RSC Advances, 2014, 4, 44654-44658.	1.7	22
85	Peroxymonosulfate activation by phosphate anion for organics degradation in water. Chemosphere, 2014, 117, 582-585.	4.2	186
86	Semiconductor heterojunction photocatalysts: design, construction, and photocatalytic performances. Chemical Society Reviews, 2014, 43, 5234.	18.7	3,257
87	Fenton-like Degradation of Reactive Dyes Catalyzed by Biogenic Jarosite. Journal of Advanced Oxidation Technologies, 2014, 17, .	0.5	0
88	Ta3N5-Pt nonwoven cloth with hierarchical nanopores as efficient and easily recyclable macroscale photocatalysts. Scientific Reports, 2014, 4, 3978.	1.6	52
89	Effects of dietary Europium complex and Europium(III) on cultured pearl colour in the pearl oyster <i>Pinctada martensii</i> . Aquaculture Research, 2013, 44, 1300-1306.	0.9	9
90	p-Nitrophenol Enhanced Degradation in High-Voltage Pulsed Corona Discharges Combined with Ozone System. Plasma Chemistry and Plasma Processing, 2013, 33, 1053-1062.	1.1	13

#	Article	IF	CITATIONS
91	Surface decoration of Bi2WO6 superstructures with Bi2O3 nanoparticles: an efficient method to improve visible-light-driven photocatalytic activity. CrystEngComm, 2013, 15, 9011.	1.3	75
92	Bioleaching of Arsenic-Rich Gold Concentrates by Bacterial Flora before and after Mutation. BioMed Research International, 2013, 2013, 1-10.	0.9	6
93	Construction of 980 nm laser-driven dye-sensitized photovoltaic cell with excellent performance for powering nanobiodevices implanted under the skin. Journal of Materials Chemistry, 2012, 22, 18156.	6.7	26
94	A Highly Sensitive Electrochemical Impedance Spectroscopy Immunosensor for Determination of 1â€Pyrenebutyric Acid Based on the Bifunctionality of Nafion/Gold Nanoparticles Composite Electrode. Chinese Journal of Chemistry, 2012, 30, 1155-1162.	2.6	11
95	Electrochemical synthesis of silver nanoparticles-coated gold nanoporous film electrode and its application to amperometric detection for trace Cr(VI). Science China Chemistry, 2011, 54, 1004-1010.	4.2	18
96	Sensitive Voltammetric Detection of Trace Heavy Metals in Real Water Using Multi-Wall Carbon Nanotubes/Nafion Composite Film Electrode. Chinese Journal of Chemistry, 2011, 29, 805-812.	2.6	28
97	A Simple and Sensitive Method for the Detection of Trace Pb(II) and Cd(II) based on Nafionâ€coated Antimony Film Electrode. Chinese Journal of Chemistry, 2010, 28, 2287-2292.	2.6	15
98	Ferrous ions inhibit Cu uptake and accumulation via inducing iron plaque and regulating the metabolism of rice plants exposed to CuO nanoparticles. Environmental Science: Nano, 0, , .	2.2	5
99	Insights into effect of chloride ion on the degradation of 4-bromo-2-chlorophenol by sulphate radical-based oxidation process. International Journal of Environmental Analytical Chemistry, 0, , 1-15.	1.8	1